Fault-Tolerant Cooperative Control for Multiple Vehicle Systems Based on Topology Reconfiguration

Huiliao Yang, *Member, IEEE*, Bin Jiang, *Fellow, IEEE*, Hao Yang, *Senior Member, IEEE*, and Hugh H. T. Liu, *Member, IEEE*

***Abstract*—In this article, the fault-tolerant synchronization and time-varying tracking control problem is investigated for nonlinear multivehicle systems (MVSs) in the presence of partial loss-of-control-effectiveness (LoCE) faults. Based on the graph theory, a two-level fault-tolerant cooperative control framework is proposed, namely, the low-level distributed nominal control scheme and the high-level topology reconfiguration protocols. The low-level scheme is developed to guarantee system performances in the fault-free scenario. With the low-level scheme, the high-level topology reconfiguration protocols, each of which corresponds to one partial LoCE fault scenario, are then proposed to mitigate the fault impact by adjusting the underlying topology. Accordingly, without modifying the structure or the design parameter of the low-level control scheme, the proposed framework can guarantee the synchronization and tracking errors of the MVS asymptotically convergent to zero in both fault-free and fault scenarios. Finally, the effectiveness of the proposed control method is verified via a simulation study of three degree-of-freedom helicopters.**

***Index Terms*—Attitude synchronization, fault-tolerant control, multivehicle system (MVS), topology reconfiguration.**

I. Introduction

MULTIVEHICLE systems (MVSs) have drawn increasing attention for their promising potential in a variety of applications, such as environment monitoring, surveillance, rescue, and target tracking [1]. For successful implementation of MVSs, attitude alignment is a non-negligible research topic. Several control strategies [2]–[9] are proposed to synchronize the attitudes of the MVS.

Manuscript received December 27, 2019; revised May 15, 2020; accepted October 20, 2020. This work was supported in part by the National Natural Science Foundations of China under Grant 62020106003, Grant 62003130, and Grant 62073165; in part by the 111 Project under Grant B20007; and in part by the Fundamental Research Funds for the Central Universities under Grant B200201047 and Grant NZ2020003. This article was recommended by Associate Editor P. Shi. *(Corresponding author: Bin Jiang.)*

Huiliao Yang is with the College of Energy and Electrical Engineering, Hohai University, Nangjing 211100, China (e-mail: yhl19901202@126.com).

Bin Jiang and Hao Yang are with the College of Automation Engineering, Nanjing University of Aeronautics and Astronautics, Nanjing 211106, China (e-mail: binjiang@nuaa.edu.cn; haoyang@nuaa.edu.cn).

Hugh H. T. Liu is with the Institute for Aerospace Studies, University of Toronto, Toronto, ON M3H 5T6, Canada (e-mail: liu@utias.utoronto.ca).

Color versions of one or more figures in this article are available at https://doi.org/10.1109/TCYB.2020.3035557.

Digital Object Identifier 10.1109/TCYB.2020.3035557

For the synchronization of the MVS, when actuator faults occur on any vehicle, both the faulty vehicle and its neighbors might be subject to performance degradation or even instability. If not addressed properly, the actuator fault impact would be propagated to the entire MVS, thereby resulting in even worse effects. Therefore, the research on fault-tolerant control schemes for MVSs is of necessity and significance. Along this topic, there already exists some literature. In [10] and [11], multilevel hierarchical frameworks are employed for the fault-tolerant cooperative control (FTCC) of linear MVSs with loss-of-control-effectiveness (LoCE) faults by using absolute and relative measurements, respectively. A similar framework is adopted in [12] to address the optimal fault recovery for linear time-invariant (LTI) MVSs. Semidecentralized optimal control strategy [13], fault compensation schemes based on fault diagnosis or estimation [14]–[18], and the decentralized adaptive fuzzy approximation method [19] are several alternatives for fault-tolerant control of linear MVSs. The robust adaptive control-based fault-tolerant control methodologies in [20] and [21] are developed for nonlinear second-order MVSs. Notably, all the aforementioned publications are developed from the fundamental fault-tolerant control technologies for individual systems. The fault-tolerant control objective is achieved by either reconfiguring controllers with accurate fault detection mechanisms or utilizing strongly robust control methodologies. It may lead to the equipment of complicated control mechanisms for implementation. Alternatively, we may wonder if fault-tolerant control strategies could be designed by utilizing unique features of MVSs.

As the most distinct property of multiple systems compared with the individual one, the topology of an MVS reflects the relations of vehicles [22]. Topology/formation reconfiguration algorithms have been proposed to withstand noise [23], improve system controllability [24], plan vehicle motion [25], and solve task assignment problems [26], [27] for MVSs. It is found that the common operations of reconfiguring or adjusting a topology include leader selection [23], weight adjustment [24], edge swapping [27], etc.

In light of these results, taking full advantage of topology should be a promising potential solution to the fault-tolerant control problem for MVSs [28]. Specifically, it presents a possibility to handle actuator faults of the MVS, such as partial LoCE faults by reconfiguring the topology/formation rather than the structure or the design parameter of the control

scheme. Along this orientation, few results have been obtained. In [29], a neighboring rule-based linear cooperative protocol is proposed for nonlinear MVSs to achieve the time-invariant target aggregation mission. By adjusting some weights of the cooperative protocol, the target point is reached even in the presence of actuator faults. In [30], a cooperative actuator fault accommodation strategy is proposed for LTI MVSs by reconfiguring the weights of agents. The FTCC method based on the plugging operations is proposed in [31] for the consensus of MVSs. In [32], vehicles with severe actuator faults are forced to get out the team, and the remaining healthy robots would be rearranged to complete the mission with performance degradation. Due to the varieties of tasks and fault types, it is difficult to provide a universal topology reconfiguration-based FTCC framework for MVSs and, thus, the focused fault-tolerant time-varying tracking control problem based on topology reconfiguration deserves to be further investigated.

Motivated by the above analysis, this work investigates the fault-tolerant synchronization and time-varying tracking control problem for the leader-following nonlinear MVS with partial LoCE faults. To solve this problem, an integrated topology reconfiguration-based FTCC framework, the diagram of which is shown in Fig. 1, is proposed. The main contributions of this article are summarized as follows.

1) The proposed integrated FTCC framework is hierarchical, and it consists of the low-level distributed nominal control scheme and the high-level topology reconfiguration protocols. The low-level scheme is developed by utilizing the state-feedback control technique to guarantee system performance in the fault-free scenario. Based on the low-level scheme, four high-level topology reconfiguration protocols are proposed to ensure the fault-tolerant ability of the MVS.
2) Each of the high-level topology reconfiguration protocols corresponds to one fault scenario. By purely conducting topology adjustment operations, it can mitigate the impact of partial LoCE faults. Therefore, only the underlying topology is adjusted by employing the proposed FTCC framework, and the structure or the design parameter of the nominal control scheme does not need to be modified. All of these features make the FTCC framework more implementation-friendly.
3) The theoretical condition that the connection weights should satisfy is given for each topology reconfiguration protocol to guarantee system performance in the corresponding fault scenario. By synthesizing these conditions, the proposed FTCC framework can ensure that the MVS achieves the attitude synchronization and asymptotically tracks the time-varying reference signals in various fault scenarios.

The remainder of this article is organized as follows. Section II presents necessary mathematical preliminaries and problem formulation. The low-level nominal control scheme and the high-level topology reconfiguration protocols for different fault scenarios are developed in Sections III and IV with rigorous stability analysis, respectively. Accordingly, the integrated topology reconfiguration-based FTCC framework is summarized in Section V. In Section VI, a simulation study on three degree-of-freedom (3-DOF) helicopters with the consideration of different fault cases is conducted. Some conclusions are drawn in Section VII.

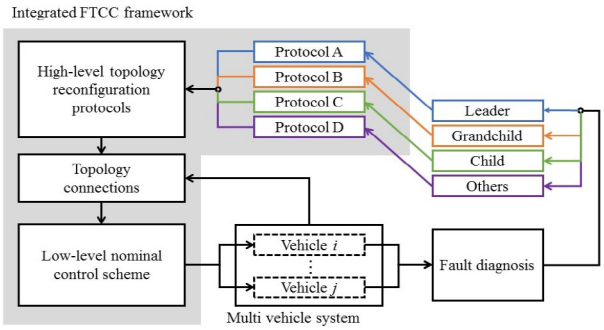

Fig. 1. Hierarchical FTCC framework for the MVS.

II. Preliminaries

A. Notations

The following notations are used in this article. For a square matrix $A \in \mathbb{R}^{n\times n}$, $(A)_{n-w} \in \mathbb{R}^{(n-w)\times(n-w)}$ represents its minor matrix by removing the first w row–column pairs ($1 \le w \le n-1$). For a nonempty set $\mathcal{S}$ and its subset $\mathcal{L}$, $\mathcal{S}/\mathcal{L}$ represents a subset of $\mathcal{S}$ by removing the set $\mathcal{L}$. For a square matrix $B \in \mathbb{R}^{n\times n}$, $\lambda_k\{B\}$, $\lambda_{\min}\{B\}$, and $\lambda_{\max}\{B\}$ represent the kth, the minimal, and the maximum eigenvalues of B, respectively, with $k = 1, 2, \ldots, n$. Let I_n be an $n \times n$ identity matrix and $1_n \in \mathbb{R}^n$ be a vector of all ones. The symbol $\otimes$ represents the Kroneker product of matrices. $\mathbb{N}_+$ denotes the set of positive integers.

B. Graph Theory

In this work, an MVS is originally considered as an undirected spanning tree. The undirected spanning tree $\mathcal{G} \triangleq [\mathcal{V}, \mathcal{E}]$ consists of nodes $\mathcal{V} = \{1, 2, \ldots, n\}$ and undirected arcs $\mathcal{E} = \{\mathcal{E}^1, \ldots, \mathcal{E}^m\}$, where $1, 2, \ldots, n$ represent the identities (IDs) of nodes. Each arc is a pair of nodes denoted as $[i, j] \in \mathcal{E}$ which implies that nodes i and j can receive information directly from each other. The neighbor set of node i, denoted as $\mathcal{N}_i \triangleq \{j \in \mathcal{V} | [j, i] \in \mathcal{E}\}$, consists of all the agents directly connected to node i. In general, tree $\mathcal{G}$ is described by a weighted adjacency matrix $A = [a_{ij}]$, where the weight a_{ij} represents the influence strength of node j on node i, and $a_{ij} > 0$ if $[i, j] \in \mathcal{E}$; otherwise, $a_{ij} = 0$. Moreover, a_{ii} is supposed to be 0 for all $i \in \mathcal{V}$. The degree matrix of $\mathcal{G}$ is denoted as $D = \text{diag}\{d_i\}$, where $d_i = \sum_{j\in\mathcal{N}_i} a_{ij}$. Therefore, the Laplacian matrix is defined as $L = D - A$. An undirected path from node 1 to node k in $\mathcal{G}$ is defined as a sequence of arcs $[1, 2], [2, 3], \ldots, [(k-1), k]$, where node $s \in \mathcal{V}$ and arc $[s, (s+1)] \in \mathcal{E}$ with $s = 1, \ldots, k-1$. In addition, the directed arc (i, j) is defined, and it represents a unidirectional connection from node i to node j, which implies j can receive information from i. Then, the corresponding directed path is defined similarly to the undirected one.

In terms of the undirected spanning tree of concern, one node is selected as the single root of this tree. Accordingly, the tree is divided into several layers in light of each node's path

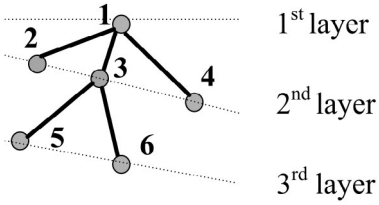

Fig. 2. Example for the undirected spanning tree.

with respect to the root. The root, the ID of which is denoted as 1, is the only node in the first layer. It is also considered as the leader of this group. In the second layer, there are nodes directly connected with the root. Furthermore, in the ath ($a \in \{\mathbb{N}_+/\{1\}\}$) layer, there are nodes which reach the root through $a-1$ arcs. They are also defined as the $(a-1)$-neighbors of the root. A node b ($b \in \mathcal{V}$) in the ath layer represents the father node of nodes in the $(a+1)$th layer that can directly receive the information from it. For example, as seen in Fig. 2, node 3 is the father node of node 5 and node 6. Conversely, a node d ($d \in \mathcal{V}$) in the $(a+1)$th layer that can directly receive the information from b represents one of its child nodes. b is denoted as $\mathcal{F}_a(d)$, and the set of its child nodes is denoted as $\mathcal{C}_h(b)$. Each node except the root has a unique father node. Furthermore, an assumption on the communication range for the considered tree should be satisfied.

Assumption 1: For the considered undirected spanning tree $\mathcal{G}$, the largest achievable communication range is the distance between node i and its farthest 2-neighbor node, where $\forall i \in \mathcal{V}$. Moreover, for each node in the fourth layer, it is always within the communication range of a node in the third layer except its own father node.

Remark 1: It is known that each node has a communication range and cannot sense nodes outside of this range. For the MVS, there always exists the largest achievable communication range between nodes. To provide more redundancy for graph connectivity but not increase the communication burden especially in fault scenarios, the assumption on the largest achievable communication range guarantees that at least one of the 2-neighbor nodes of the faulty vehicle would be within its communication range. Meanwhile, the extra assumption on the communication capability of each node in the fourth layer is also made to ensure topology reconfiguration protocols proposed later in Section IV executable.

C. Problem Formulation

The general affine nonlinear model of the ith vehicle is given by [33]

$$\begin{cases} \dot{x}_i(t) = v_i(t) \\ \dot{v}_i(t) = f(x_i) + g(x_i)u_i \end{cases} \tag{1}$$

where $x_i, v_i \in \mathbb{R}^N$ represent the position/attitude and its rate of the ith vehicle with $i = 1, \ldots, n$ ($n \geq 3$), respectively. The control input vector is denoted as $u_i(\cdot) \in \mathbb{R}^m$. $f(x_i)$ and $g(x_i)$ are the known vector and invertible matrix with appropriate dimensions, respectively.

Accordingly, the model of the entire MVS is described as

$$\begin{cases} \dot{x}(t) = v(t) \\ \dot{v}(t) = F(x) + G(x)U \end{cases} \tag{2}$$

where $x = [x_1^\mathsf{T}, \ldots, x_n^\mathsf{T}]^\mathsf{T}$ and $v = [v_1^\mathsf{T}, \ldots, v_n^\mathsf{T}]^\mathsf{T}$ are the states of the MVS. $F(x) = [f^\mathsf{T}(x_1), \ldots, f^\mathsf{T}(x_n)]^\mathsf{T}$, $G(x) = \text{diag}\{g(x_1), \ldots, g(x_n)\}$, and $U = [u_1^\mathsf{T}, \ldots, u_n^\mathsf{T}]^\mathsf{T}$.

Suppose that partial LoCE faults occur on the ith vehicle's actuators, and then the model in (1) changes into the following form:

$$\begin{cases} \dot{x}_i(t) = v_i(t) \\ \dot{v}_i(t) = f(x_i) + g(x_i)\rho_i(t)u_i \end{cases} \tag{3}$$

where $\rho_i = \text{diag}\{\rho_{i1}, \ldots, \rho_{im}\}$ with $0 < \rho_{ik} \leq 1$, $i = 1, \ldots, n$ and $k = 1, \ldots, m$. ρ_{ik} indicates the remaining effectiveness of the kth control signal of the ith vehicle. It is notable that if the partial LoCE fault occurs on the kth control channel of the ith vehicle at time instant t_f and is detected at time instant t_d ($t_d > t_f > 0$), it should not jump into another mode during the interval $[t_f, t_s]$, where t_s ($t_s > t_d$) is another time instant and $t_s - t_d$ should be sufficiently large.

Then, the model of the entire MVS in (2) is replaced by the following description:

$$\begin{cases} \dot{x}(t) = v(t) \\ \dot{v}(t) = F(x) + G(x)\Gamma U \end{cases} \tag{4}$$

with $\Gamma = \text{diag}\{I_{(i-1)m}, \ldots, \rho_i, I_{(n-i)m}\}$ and $i = 1, \ldots, n$.

In this work, each vehicle is required to track the reference signals obtained by the following generator:

$$\begin{cases} \dot{x}_r(t) = v_r(t) \\ \dot{v}_r(t) = f(x_r) \end{cases} \tag{5}$$

where $x_r,\ v_r \in \mathbb{R}^N$ are reference signals of states. Therefore, the control objective is descried as follows.

Problem: Under the FTCC framework shown in Fig. 1, design the nominal control scheme and the topology reconfiguration protocols for the MVS (4) considering partial LoCE faults. As a result, for the reference signals x_r and v_r generated by (5), the synchronization errors $x_i - x_j$, $v_i - v_j$ with $i \in \mathcal{V}$, $j \in \mathcal{N}_i$ and the tracking errors $x_i - x_r$, $v_i - v_r$ with $i \in \mathcal{V}$ can asymptotically converge to 0. Meanwhile, in both the fault-free and fault scenarios, the nominal control scheme can maintain the original structure and design parameter.

For the model of the ith vehicle shown in (1), denote $f(x_i)$ as $f(x_i) = [f_1(x_i), \ldots, f_N(x_i)]^\mathsf{T}$, and then we have the following assumption.

Assumption 2: For the system nonlinearity shown in (1), it should satisfy the following Lipschitz condition:

$$|f_k(x_i) - f_k(y_i)| \leq l_{ik}|x_{ik} - y_{ik}|$$

where $x_i,\ y_i \in \mathbb{R}^N$, and $x_{ik},\ y_{ik}$ are their kth elements, respectively, with $k = 1, \ldots, N$. l_{ik} are constants with $i = 1, \ldots, n$.

To proceed the development of the FTCC framework, the following lemmas would be applied in our work.

Lemma 1 [34]: If Q and E are $n \times n$ symmetric matrices, we have $\lambda_{\min}\{Q\} + \lambda_{\min}\{E\} \leq \lambda_i\{S\} \leq \lambda_{\max}\{Q\} + \lambda_{\max}\{E\}$ with $S = Q + E$ and $i = 1, \ldots, n$.

Lemma 2 [35]: Let M denote an $n \times n$ ($n \geq 2$) Hermitian matrix whose entries are in the interval $[a,\ b]$. If $a \geq -|b|$, we have $\lambda_{\max}\{M\} \leq nb$.

Overall, the investigated control problem prefers to be solved by adjusting the topology of the MVS rather than modifying the structure or the design parameter of the nominal control scheme like the conventional methods, such as [14]. It is notable that nonlinear MVSs with general forms instead of the LTI ones [30] are studied. Furthermore, the faults considered are more common and of physical significance in real applications compared with [29] and [31].

III. Low-Level Nominal Control Design

For the spanning tree $\mathcal{G}$, generally, only the leading vehicle has the access to the reference signals generated by (5). Accordingly, the distributed nominal control scheme based on the state-feedback control is developed as follows.

1) For the leading vehicle, the control law is designed as

$$u_1 = g_i^{-1}\left(-c\sum_{j\in\mathcal{N}_1} a_{ij}\big((x_1 - x_j) + (v_1 - v_j)\big) - b_1((x_1 - x_r) + (v_1 - v_r))\right) \tag{6}$$

where $c > 0$ is a design parameter, and b_1 satisfies $b_1 > 0$ and is usually called the pinning gain [34].

2) For the following vehicle i ($i \in \{\mathcal{V}/\{1\}\}$), the control law is designed as:

$$u_i = g_i^{-1}\left(-c\sum_{j\in\mathcal{N}_i} a_{ij}\big((x_i - x_j) + (v_i - v_j)\big)\right). \tag{7}$$

According to Assumption 2, a positive gain p is defined as follows:

$$p = \max_{1\leq i\leq n,\ 1\leq k\leq N}\left\{\left(l_{ik} + 0.5l_{ik}^{2(1-\sigma)}\right),\ \left(0.5l_{ik}^{2\sigma} + 1\right)\right\} \tag{8}$$

with $0 \leq \sigma \leq 1$. It is obvious that $p \geq 1$, and this property will be utilized in the stability analysis later soon.

Construct the following symmetric matrix:

$$H = cL - pI_n \tag{9}$$

where $L \in \mathbb{R}^{n\times n}$ is the Laplacian matrix of the MVS. Let $B \in \mathbb{R}^{n\times n} = \text{diag}\{b_1, 0\ldots, 0\}$ denote the pinning matrix, then we have

$$H + B = \begin{bmatrix} c\sum\limits_{j\in\mathcal{N}_1} a_{1j} - p + b_1 & D \\ D^{\mathsf{T}} & (H)_{n-1} \end{bmatrix}$$

where $(H)_{n-1} = (cL - pI_n)_{n-1}$. D^{T} is a vector with proper columns. Due to space limitations, the expression of D^{T} is omitted.

Then, the stability conditions of the MVS under the developed nominal control laws are demonstrated in the following theorem.

Theorem 1: For the MVS (4) with $\Gamma = I_{nm}$, design the topology as an undirected spanning tree and the control laws as (6) and (7). If the design parameter c, the pinning gain b_1, and all the connection weights a_{ij} with $i \in \mathcal{V}$, $j \in \mathcal{N}_i$ are set to satisfy the following two conditions:

$$b_1 > p - c\sum_{j\in\mathcal{N}_1} a_{1j} \tag{10}$$

$$\lambda_{\min}\{(L)_{n-1}\} > \frac{(n-1)\max_{j\in\mathcal{N}_1}\ a_{1j}^2}{\sum_{j\in\mathcal{N}_1} a_{1j} + \frac{b_1 - p}{c}} + \frac{p}{c} \tag{11}$$

then the states x and v of this system can asymptotically track the reference signals x_r and v_r generated by (5), respectively.

Proof: Let $\tilde{x} = x - 1_n \otimes x_r$ and $\tilde{v} = v - 1_n \otimes v_r$. With $\Gamma = I_{nm}$, the model of the entire MVS in (4) under the nominal control laws (6) and (7) can be rewritten as follows:

$$\begin{cases} \dot{\tilde{x}}(t) = \tilde{v}(t) \\ \dot{\tilde{v}}(t) = -((cL + B)\otimes I_N)(\tilde{x} + \tilde{v}) \\ \qquad\quad + F(x) - 1_n \otimes f(x_r). \end{cases}$$

Define the following matrix:

$$P = \begin{bmatrix} 2(cL + B) & I_n \\ I_n & I_n \end{bmatrix}.$$

1) Validity of P: First, we evaluate whether P is positive definite, that is, $P > 0$. With the Schur complement, it can be obtained that $P > 0$ is equivalent to $cL + B - 0.5I_n > 0$. Condition (11) implies that $c\lambda_{\min}\{(L)_{n-1}\} - p > 0$. By utilizing Lemma 1, we have $\lambda_{\min}\{(cL - pI)_{n-1}\} \geq c\lambda_{\min}\{(L)_{n-1}\} - p > 0$, which indicates that $(H)_{n-1} > 0$. In view of conditions (10), (11) and the Schur complement, we have $cL - pI_n + B > 0$. Since $p \geq 1$, it is proved that $P > 0$.

2) Stability: Let $\tilde{y} = [\tilde{x}^{\mathsf{T}}, \tilde{v}^{\mathsf{T}}]^{\mathsf{T}}$. With the positive-definite matrix P, we design the following Lyapunov candidate as $V = 0.5\tilde{y}^{\mathsf{T}}(P \otimes I_N)\tilde{y}$.

Taking the time derivative of V yields

$$\begin{aligned} \dot{V} &= \tilde{x}^{\mathsf{T}}(2(cL + B)\otimes I_N)\tilde{v} + \tilde{v}^{\mathsf{T}}\tilde{v} \\ &\quad + \left(\tilde{x}^{\mathsf{T}} + \tilde{v}^{\mathsf{T}}\right)(-(cL + B)\otimes I_N)(\tilde{x} + \tilde{v}) \\ &\quad + \left(\tilde{x}^{\mathsf{T}} + \tilde{v}^{\mathsf{T}}\right)(F(x) - 1_n \otimes f(x_r)) \\ &\leq \tilde{x}^{\mathsf{T}}((qI_n - cL - B)\otimes I_N)\tilde{x} \\ &\quad + \tilde{v}^{\mathsf{T}}((rI_n - cL - B)\otimes I_N)\tilde{v} \end{aligned}$$

with

$$q = \max_{1\leq i\leq n,\ 1\leq k\leq N}\left\{\left(l_{ik} + 0.5l_{ik}^{2(1-\sigma)}\right)\right\}$$

$$r = \max_{1\leq i\leq n,\ 1\leq k\leq N}\left\{\left(0.5l_{ik}^{2\sigma} + 1\right)\right\}.$$

It has been verified that $cL - pI_n + B > 0$. Accordingly, it is easy to conclude that $qI_n - cL - B < 0$ and $rI_n - cL - B < 0$. Thus, we have $\dot{V} \leq 0$ and $\dot{V} = 0$ if and only if $\tilde{x} = 0$ and $\tilde{v} = 0$. Based on LaSalle's invariant principle [36], it is further obtained that $V \to 0$ as $t \to \infty$, that is, $\|\tilde{x}\| \to 0$ and $\|\tilde{v}\| \to 0$ as $t \to \infty$. Therefore, the considered MVS can globally asymptotically track the reference signals in a synchronized way. This completes the proof. ■

From the above proof, it is found that the selection of the connection weights, the design parameter and the pinning gain can directly affect the stability of the MVS. Theorem 1

provides a guideline to design the connection weights of the original topology. If the weights a_{1j} of the connections between the leader and its followers are designed as small scalars, it means that the leader itself might not be able to provide enough effort to "drag" the followers. Thus, the design parameter c and the pinning gain b_1 should be relatively large to guarantee the system performance. On the other hand, if a_{1j} are set as large scalars, it means that the connections between the leader and followers become more tight. Consequently, b_1 should be large enough such that more power can be provided to drag both the leader and followers. Therefore, a_{1j}, c, and b_1 should be selected properly to decrease the energy consumption.

IV. High-Level Topology Reconfiguration Protocols Under Different Fault Scenarios

In this section, we explore how to tolerate the faulty vehicles by adjusting some connection weights or modifying connections in different fault scenarios.

Under the nominal control laws (6) and (7), the model of the MVS considering LoCE faults in (4) is rewritten as

$$\begin{cases} \dot{\tilde{x}}(t) = \tilde{v}(t) \\ \dot{\tilde{v}}(t) = -G(x)\Gamma G^{-1}(x)((cL+B)\otimes I_N)(\tilde{x}+\tilde{v}) \\ \qquad + F(x) - 1_n \otimes f(x_r). \end{cases}$$

Before going any further steps, an assumption for the LoCE fault is made as follows.

Assumption 3: For Γ, there exists an unknown but detectable constant $\rho_0 > 0$ such that $\rho_0 I_{Nn} \le \Gamma < I_{Nn}$.

Now, label the faulty vehicle as h ($h \in \mathcal{V}$), and then we define matrices $\bar{B}$ and $\bar{L}$ which can be considered as the new pinning and Laplacian matrices of the faulty MVS, respectively. Their expressions are shown as follows:

$$\begin{aligned} \bar{B} &\triangleq \bar{\rho}_0 B \\ \bar{L} &\triangleq \bar{\rho}_0 L \end{aligned} \tag{12}$$

with $\bar{\rho}_0 = \mathrm{diag}\{I_{h-1}, \rho_0, I_{n-h}\}$.

Recall (9) and construct the following symmetric matrix in a similar formula:

$$\bar{H} = 0.5c\left(\bar{L} + \bar{L}^{\mathsf{T}}\right) - pI_n.$$

Then, we will develop the detailed topology reconfiguration protocols and analyze the stability of the MVS in the scenarios where the leader, its grandchild and child nodes, and other nodes are faulty in Sections IV-A–IV-D, respectively.

A. Protocol A: The Leader Is Faulty

Consider the scenario in which the leader is faulty, that is, $h = 1$. Then, we have $\bar{\rho}_0 = \mathrm{diag}\{\rho_0, I_{n-1}\}$, and the Laplacian matrix in (12) is rewritten as

$$\bar{L} = \begin{bmatrix} \rho_0 \sum\limits_{j\in\mathcal{N}_1} a_{1j} & -\rho_0 a_{12} & \cdots & -\rho_0 a_{1n} \\ -a_{21} & \sum\limits_{j\in\mathcal{N}_2} a_{2j} & \cdots & -a_{2n} \\ \vdots & \vdots & \ddots & \vdots \\ -a_{n1} & -a_{n2} & \cdots & \sum\limits_{j\in\mathcal{N}_n} a_{nj} \end{bmatrix}.$$

With the fact that $a_{1j} = a_{j1}$, the following equation can be obtained:

$$\begin{aligned} &0.5\left(\bar{L} + \bar{L}^{\mathsf{T}}\right) \\ &= \begin{bmatrix} \rho_0 \sum\limits_{j\in\mathcal{N}_1} a_{1j} & -\frac{\rho_0+1}{2} a_{12} & \cdots & -\frac{\rho_0+1}{2} a_{1n} \\ -\frac{\rho_0+1}{2} a_{21} & \sum\limits_{j\in\mathcal{N}_2} a_{2j} & \cdots & -a_{2n} \\ \vdots & \vdots & \ddots & \vdots \\ -\frac{\rho_0+1}{2} a_{n1} & -a_{n2} & \cdots & \sum\limits_{j\in\mathcal{N}_n} a_{nj} \end{bmatrix}. \end{aligned} \tag{13}$$

Then, we have

$$\bar{H} + \bar{B} = \begin{bmatrix} \rho_0\left(c\sum\limits_{j\in\mathcal{N}_1} a_{1j} + b_1\right) - p & \bar{D} \\ \bar{D}^{\mathsf{T}} & \left(\bar{H}\right)_{n-1} \end{bmatrix}$$

where $\bar{D}^{\mathsf{T}}$ denotes a vector with proper columns, and its expression is omitted as well.

Seeing from the above equation, we find that increasing the pinning gain b_1 can mitigate the LoCE fault impact. Accordingly, tune b_1 as the following new pinning gain:

$$\bar{b}_1 = \frac{1}{\rho_0} b_1 + \frac{1-\rho_0}{\rho_0} c \sum_{j\in\mathcal{N}_1} a_{1j}$$

where ρ_0 is obtained from the fault detection. Then, we have the following theorem.

Theorem 2: For the MVS (4) with $\Gamma = I_{nm}$, design the original topology and nominal control laws (6) and (7) to satisfy Theorem 1. When the leading vehicle in this group suffers the partial LoCE faults described in (3) that satisfy Assumption 3, by tuning the pinning gain b_1 as $\bar{b}_1$, the faulty MVS (4) can asymptotically track the references x_r and v_r generated by (5) with the original structure and design parameter of nominal control laws in spite of the faulty leader.

Proof: First, define the matrix $\bar{P}$ as follows:

$$\bar{P} = \begin{bmatrix} c\left(\bar{L} + \bar{L}^{\mathsf{T}}\right) + 2\tilde{B} & I_n \\ I_n & I_n \end{bmatrix}$$

where $\tilde{B} = \bar{\rho}_0 \mathrm{diag}\{\bar{b}_1, 0, \ldots, 0\}$ is the updated pinning matrix.

1) Validity of $\bar{P}$: We check whether $\bar{P}$ is positive definite. In light of the Schur complement, $\bar{P} > 0$ is equivalent to $0.5c(\bar{L} + \bar{L}^{\mathsf{T}}) + \tilde{B} - 0.5I_n > 0$.

It is easily obtained that

$$\bar{H} + \tilde{B} = \begin{bmatrix} \rho_0\left(c\sum\limits_{j\in\mathcal{N}_1} a_{1j} + \bar{b}_1\right) - p & \bar{D} \\ \bar{D}^{\mathsf{T}} & \left(\bar{H}\right)_{n-1} \end{bmatrix}.$$

Based on the expression of $\bar{b}_1$, the following inequality holds:

$$\rho_0\left(c\sum_{j\in\mathcal{N}_1} a_{1j} + \bar{b}_1\right) - p = c\sum_{j\in\mathcal{N}_1} a_{1j} - p + b_1 > 0. \tag{14}$$

Considering (13), we have $(\bar{H})_{n-1} = (H)_{n-1}$ and

$$\lambda_{\min}\left\{\left(0.5\left(\bar{L} + \bar{L}^{\mathsf{T}}\right)\right)_{n-1}\right\} = \lambda_{\min}\{(L)_{n-1}\}.$$

Then, it yields

$$\begin{aligned}&\lambda_{\max}\left\{\bar{D}^{\mathsf{T}}\left(\rho_0\left(c\sum_{j\in\mathcal{N}_1}a_{1j}+\bar{b}_1\right)-p\right)^{-1}\bar{D}\right\}\\&\le\frac{(1+\rho_0)^2}{4}\frac{(n-1)\max_{j\in\mathcal{N}_1}a_{1j}^2}{\sum_{j\in\mathcal{N}_1}a_{1j}+\frac{b_1-p}{c}}+\frac{p}{c}\\&\le\lambda_{\min}\{(L)_{n-1}\}=\lambda_{\min}\left\{\left(0.5\left(\bar{L}+\bar{L}^{\mathsf{T}}\right)\right)_{n-1}\right\}.\end{aligned}\tag{15}$$

By applying the Schur complement, it is proved that $\bar{P}>0$.

2) Stability: With the positive-definite matrix $\bar{P}$, another Lyapunov candidate is designed as $\bar{V}=0.5\tilde{y}^{\mathsf{T}}(\bar{P}\otimes I_N)\tilde{y}$.

By taking the time derivative of $\bar{V}$, we have

$$\begin{aligned}\dot{\bar{V}}&=\tilde{x}^{\mathsf{T}}\left(\left(c\left(\bar{L}+\bar{L}^{\mathsf{T}}\right)+2\tilde{B}\right)\otimes I_N\right)\tilde{v}+\tilde{v}^{\mathsf{T}}\tilde{v}\\&\quad+\left(\tilde{x}^{\mathsf{T}}+\tilde{v}^{\mathsf{T}}\right)\left(-G(x)\rho G^{-1}(x)\hat{H}(\tilde{x}+\tilde{v})\right)\\&\quad+\left(\tilde{x}^{\mathsf{T}}+\tilde{v}^{\mathsf{T}}\right)(F(x)-1_n\otimes f(x_r))\\&\le\tilde{x}^{\mathsf{T}}\left(\left(qI_n-0.5c\left(\bar{L}+\bar{L}^{\mathsf{T}}\right)-\tilde{B}\right)\otimes I_N\right)\tilde{x}\\&\quad+\tilde{v}^{\mathsf{T}}\left(\left(rI_n-0.5c\left(\bar{L}+\bar{L}^{\mathsf{T}}\right)-\tilde{B}\right)\otimes I_N\right)\tilde{v}\end{aligned}\tag{16}$$

where $\hat{H}=(cL+\hat{B})\otimes I_N$ with $\hat{B}=\mathrm{diag}\{\bar{b}_1,0,\ldots,0\}$.

Similarly, with Conditions (14) and (15), we can conclude that $\dot{\bar{V}}(t)\le 0$, and $\dot{\bar{V}}=0$ if and only if $\tilde{x}=0$ and $\tilde{v}=0$. Furthermore, based on LaSalle's invariant principle, the tracking errors $\tilde{x}$ and $\tilde{v}$ of the entire group are guaranteed to be globally asymptotically convergent to zero in this scenario. This completes the proof. ■

B. Protocol B: A Grandchild Node of the Leader Is Faulty

Consider the scenario in which a grandchild node of the leader is faulty, and then the Laplacian matrix in (12) is rewritten as

$$\bar{L}=\begin{bmatrix}\sum\limits_{j\in\mathcal{N}_1}a_{1j}&\cdots&0&\cdots&-a_{1n}\\\vdots&\ddots&\vdots&\vdots&\vdots\\0&\cdots&\rho_0\sum\limits_{j\in\mathcal{N}_h}a_{hj}&\cdots&-\rho_0a_{hn}\\\vdots&\vdots&\vdots&\ddots&\vdots\\-a_{n1}&\cdots&-a_{nh}&\cdots&\sum\limits_{j\in\mathcal{N}_n}a_{nj}\end{bmatrix}.$$

Seeing from the stability results in the fault-free scenario, we find that apart from tuning the pinning gain as in protocol A, modifying the connections has the potential to deal with faults. Specifically, in this scenario, increasing the in-degree [30] of the faulty vehicle h, that is, adding new connections flowing into h, can bring about more control effort to mitigate the LoCE fault impact. Based on the above equation, we build a directed arc from 1 to h with $a_{h1}=2\max_{k\in\mathcal{N}_1}a_{1k}$. Then, the original connection weights a_{jh} are adjusted as $\bar{a}_{jh}$ with $\bar{a}_{jh}=(2-\rho_0)a_{jh}$ and $j\in\mathcal{N}_h$. As a consequence, the following matrix $\tilde{L}$ is defined as the updated Laplacian matrix after conducting these connection adjustments:

$$\tilde{L}=\begin{bmatrix}\sum\limits_{j\in\mathcal{N}_1}a_{1j}&\cdots&0&\cdots&-a_{1n}\\\vdots&\ddots&\vdots&\vdots&\vdots\\-\rho_0a_M&\cdots&\bar{a}_{hh}&\cdots&-\rho_0a_{hn}\\\vdots&\vdots&\vdots&\ddots&\vdots\\-a_{n1}&\cdots&-(2-\rho_0)a_{nh}&\cdots&\bar{a}_{nn}\end{bmatrix}$$

where $\bar{a}_{hh}=\rho_0(\sum_{j\in\mathcal{N}_h}a_{hj}+a_M)$ and $\bar{a}_{pp}=\sum_{j\in\mathcal{N}_p}a_{pj}+(1-\rho_0)a_{ph}$ with $p\in\{\mathcal{V}/\{1,h\}\}$.

Accordingly, we also have

$$\begin{aligned}&0.5\left(\tilde{L}+\tilde{L}^{\mathsf{T}}\right)\\&=\begin{bmatrix}\sum\limits_{j\in\mathcal{N}_1}a_{1j}&\cdots&-0.5\rho_0a_M&\cdots&-a_{1n}\\\vdots&\ddots&\vdots&\vdots&\vdots\\-0.5\rho_0a_M&\cdots&\bar{a}_{hh}&\cdots&-a_{hn}\\\vdots&\vdots&\vdots&\ddots&\vdots\\-a_{n1}&\cdots&-a_{nh}&\cdots&\bar{a}_{nn}\end{bmatrix}.\end{aligned}\tag{17}$$

Then, the following theorem is obtained.

Theorem 3: For the MVS (4) with $\Gamma=I_{nm}$, design the original topology and nominal control laws (6) and (7) to satisfy Theorem 1 and Assumption 1. Consider the scenario where a grandchild node h of the leader suffers the partial LoCE faults described in (3), the maximum tolerable magnitude of which satisfies the following inequality:

$$1-\rho_0\le\frac{a_M}{\sum_{j\in\mathcal{N}_h}a_{hj}+a_M}\tag{18}$$

where $a_M\triangleq\max_{k\in\mathcal{N}_1}a_{1k}$. By building a new directed arc from 1 to h, the weight of which is set as $a_{h1}=2a_M$, and adjusting the weights a_{jh} ($j\in\mathcal{N}_h$) as $\bar{a}_{jh}=(2-\rho_0)a_{jh}$, the faulty MVS (4) can asymptotically track the references x_r and v_r generated by (5) with the original structure and design parameter of nominal control laws in spite of the faulty vehicle.

Proof: Define the following matrix $\tilde{P}$ as:

$$\tilde{P}=\begin{bmatrix}c\left(\tilde{L}+\tilde{L}^{\mathsf{T}}\right)+2\bar{B}&I_n\\I_n&I_n\end{bmatrix}.\tag{19}$$

1) Validity of $\tilde{P}$: $\tilde{P}>0$ is equivalent to $0.5c(\tilde{L}+\tilde{L}^{\mathsf{T}})+\bar{B}-0.5I_n>0$.

Based on (17), it is not difficult to see that $c\sum_{j\in\mathcal{N}_1}a_{1j}-p+b_1>0$ holds in this scenario. Furthermore, we have

$$\begin{aligned}&\lambda_{\min}\left\{\left(0.5\left(\tilde{L}+\tilde{L}^{\mathsf{T}}\right)\right)_{n-1}\right\}\\&\ge\lambda_{\min}\{(L)_{n-1}\}+\lambda_{\min}\{\mathrm{diag}\{a_{20},\ldots,a_{n0}\}\}\end{aligned}$$

where $a_{p0}=(1-\rho_0)a_{ph}$ with $p\in\{\mathcal{V}/\{1,h\}\}$, and $a_{h0}=(\rho_0-1)\sum_{j\in\mathcal{N}_h}a_{hj}+\rho_0a_M$. With Condition (18) and Lemma 1, it is easily obtained that

$$\lambda_{\min}\left\{\left(0.5\left(\tilde{L}+\tilde{L}^{\mathsf{T}}\right)\right)_{n-1}\right\}\ge\lambda_{\min}\{(L)_{n-1}\}.$$

Similarly with (15), we have

$$\lambda_{\max}\left\{\tilde{D}^{\mathsf{T}}\left(\left(c\sum_{j\in\mathcal{N}_1}a_{1j}+b_1\right)-p\right)^{-1}\tilde{D}\right\}$$
$$\leq \lambda_{\min}\{(L)_{n-1}\}\leq \lambda_{\min}\left\{\left(0.5\left(\tilde{L}+\tilde{L}^{\mathsf{T}}\right)\right)_{n-1}\right\}$$

where $\tilde{D}^{\mathsf{T}}$ is calculated from the following definition:

$$\tilde{H}+\bar{B}=\begin{bmatrix} c\sum_{j\in N_1}a_{1j}+b_1-p & \tilde{D} \\ \tilde{D}^{\mathsf{T}} & \left(\tilde{H}\right)_{n-1}\end{bmatrix}$$

with $\tilde{H}=0.5c(\tilde{L}+\tilde{L}^{\mathsf{T}})-pI_n$. By applying the Schur complement, it is proved that $\tilde{P}$ is positive definite as well.

2) Stability: By taking the time derivative of the following Lyapunov candidate $\tilde{V}=(1/2)\tilde{y}^{\mathsf{T}}(\tilde{P}\otimes I_N)\tilde{y}$, it is not difficult to see that the tracking errors $\tilde{x}$ and $\tilde{v}$ of the MVS globally asymptotically converge to zero in this scenario. This completes the proof. ∎

From the proof of Theorem 3, it is found that if the faulty vehicle h is the grandchild of the leader, building the new directed arc $(1,h)$ can not only provide more effort to mitigate the fault impact without violating the communication constraints demonstrated in Assumption 1 but also would not affect the stability of the leader. Meanwhile, for the neighbors of h, increasing the weights a_{jh} ($j\in\mathcal{N}_h$) of the connections (h,j) as $(2-\rho_0)a_{jh}$ can exactly counteract the impact induced by node h.

Remark 2: The constraint in (18) implies that when the faulty vehicle is the grandchild of the leader, the maximum tolerable loss $(1-\rho_0)$ of control effectiveness is specified by users, and can be as large as possible if we enlarge the weight a_M in the nominal control design. It is reasonable that the tight connections between the leader and its followers can expand the fault tolerance margin of the MVS, since they can indirectly weaken the role of the faulty vehicle in the group. However, when a_M increases, the design parameter c and the pinning gain b_1 should increase accordingly to achieve the synchronized tracking. Therefore, there exists a tradeoff between the fault-tolerant ability and the energy consumption.

C. Protocol C: A Child Node of the Leader Is Faulty

For the scenario in which the vehicle directly connected with the leader is faulty, if we tune the connection weight a_{h1} and increase the in-degree of h similarly as in protocol *B*, the low-level control scheme may be unable to maintain the system stability without modifying the design parameter c. This is because the faulty vehicle would directly affect the leader in this scenario, and accordingly has more adverse impact on the entire MVS compared with the one in protocol *B*. Therefore, it may not be feasible by merely tuning connection weights and/or adding new connections to ensure the fault tolerance ability in this scenario. Alternatively, if the faulty vehicle is rearranged as one of its child node, the fault impact can be mitigated under the same topology reconfiguration protocol as in Section IV-B. Under the circumstances, node swapping between the faulty vehicle and one of its child node should be done before modifying connections. The following protocol, Algorithm 1, the computational complexity of which is $O(n)$, shows the details of node swapping and connection adjustments to achieve the fault tolerance objective. Furthermore, the swapping is accomplished with the smallest number of new connections under the communication constraints demonstrated in Assumption 1.

Algorithm 1 Node Swapping-Based Topology Reconfiguration Protocol

Input: vehicle h and the information of ρ_0;

Output: do swapping between vehicle h and a node in $\mathcal{C}_h(h)$ to achieve the fault tolerance objective;

1: select a $r\in\mathcal{C}_h(h)$ s.t. the number of nodes in $\mathcal{C}_h(r)$ is minimal;
2: delete $(h,1)$, $[h,p]$ and $[r,o]$, and simultaneously build $[1,r]$,$[r,p]$ and $[h,o]$, $\forall p\in\{\mathcal{C}_h(h)/r\}$ and $\forall o\in\mathcal{C}_h(r)$;
3: let h and r exchange their IDs;
4: set $a_{r1}=2a_M$;
5: set $\bar{a}_{jr}=(2-\rho_0)a_{jr}$, and adjust a_{jr} as $a_{jr}=\bar{a}_{jr}$, $j\in\mathcal{N}_r$

After the node swapping, the faulty vehicle becomes the grandchild node of the leader. Then, we can obtain the following theorem.

Theorem 4: For the MVS (4) with $\Gamma=I_{nm}$, design the original topology and nominal control laws (6) and (7) to satisfy Theorem 1 and Assumption 1. Consider the scenario where a child node h of the leader suffers the partial LoCE faults described in (3), the maximum tolerable magnitude of which satisfies the following inequality:

$$1-\rho_0\leq\frac{a_M}{\sum_{j\in\mathcal{N}_r}a_{rj}+a_M}\quad\forall r\in\mathcal{C}_h(h). \tag{20}$$

By conducting Algorithm 1, the faulty MVS (4) can asymptotically track the references x_r and v_r generated by (5) with the original structure and design parameter of nominal control laws in spite of the faulty vehicle.

Proof: The proof of Theorem 4 is similar to that of Theorem 3, so it is omitted here. ∎

D. Protocol D: One of the Remaining Vehicles Is Faulty

Apart from the aforementioned fault scenarios, the scenario where one of the vehicles in the kth ($k\geq 4$) layer is faulty is explored in this section.

In this case, we adopt the similar approach with protocol *B*, that is, modifying the connections via increasing the in-degree of the faulty vehicle, to mitigate the LoCE fault impact. Notably, due to the communication constraints in Assumption 1, we cannot directly add a directed arc from the leader to the faulty vehicle as in protocol *B*. Instead, a new directed path from the leader to the faulty vehicle is built. The details of this process are shown in Algorithm 2.

Based on Algorithm 2 with the computational complexity of $O(n^2)$, we can obtain the following theorem.

Theorem 5: For the MVS (4) with $\Gamma=I_{nm}$, design the original topology and nominal control laws (6) and (7) to satisfy Theorem 1 and Assumption 1. Consider the scenario where a

Algorithm 2 Protocol for Building a New Directed Path From the Leader to the Faulty Vehicle

Input: vehicle h, its layer number k and the information of ρ_0;

Output: build a new directed path from 1 to h;

```
adjust the original connection weights a_jh (j ∈ N_h) as ā_jh = (2 − ρ_0)a_jh;
q = h;
if k = 4 + 2p (p = 0, 1, 2, ...) then
    if p > 0 then
        while q is not in the 4th layer do
            build a directed arc (F_a(F_a(q)), q);
            q = F_a(F_a(q));
        end while
    end if
    select a node n in {C_h(F_a(F_a(q)))/F_a(q)}, and build directed arcs (n, q) and (1, n) simultaneously;
else
    while q is not in the 3rd layer do
        build a directed arc (F_a(F_a(q)), q);
        q = F_a(F_a(q));
    end while
    build a directed arc (1, q);
end if
```

node h in the kth ($k \geq 4$) layer suffers the partial LoCE faults described in (3), the maximum tolerable magnitude of which satisfies the following inequality:

$$1 - \rho_0 \leq \frac{2a_M}{\sum_{j\in\mathcal{N}_h} a_{hj}}. \tag{21}$$

Then, adjust the weights a_{jh} ($j \in \mathcal{N}_h$) as $\bar{a}_{jh} = (2-\rho_0)a_{jh}$, and build a new directed path from the leader to h in light of Algorithm 2, the arcs of which are denoted as $(1, h_1)$, (h_1, h_2), (h_{t-1}, h_t) ($h_t = h$, $t \in \mathbb{N}_+$). If their weights are set to satisfy the following conditions:

$$\begin{cases} a_{h_2,h_1} > \frac{2(1-\rho_0)}{\rho_0}\sum_{j\in\mathcal{N}_h} a_{hj} \\ 2a_M \geq a_{h_1,1} > 0.5\rho_0 a_{h_2,h_1} \end{cases}, \ t = 2$$

or

$$\begin{cases} a_{h_3,h_2} > \frac{2(1-\rho_0)}{\rho_0}\sum_{j\in\mathcal{N}_h} a_{hj} \\ a_{h_2,h_1} > \rho_0 a_{h_3,h_2} \\ 2a_M \geq a_{h_1,1} > 0.5a_{h_2,h_1} \end{cases}, \ t = 3$$

or

$$\begin{cases} a_{h_t,h_{t-1}} > \frac{2(1-\rho_0)}{\rho_0}\sum_{j\in\mathcal{N}_h} a_{hj} \\ a_{h_{t-1},h_{t-2}} > \rho_0 a_{h_t,h_{t-1}} \\ a_{h_{p+1},h_p} > a_{h_{p+2},h_{p+1}}, \ p = 1,\ldots,t-3 \\ 2a_M > a_{h_1,1} > 0.5a_{h_2,h_1} \end{cases}, \quad t > 3$$

the faulty MVS (4) can asymptotically track the references x_r and v_r generated by (5) in spite of the faulty vehicle.

Proof: Here, we only prove the stability of the case in which the layer number of the faulty vehicle satisfies $k = 4 + 2p$ ($p = 2, 3, \ldots$). The proof of other cases is similar and omitted accordingly.

After conducting Algorithm 2, the Laplacian matrix $\bar{L}$ in (12) is updated as a new one, denoted as $\hat{L}$, the formula of which is shown on the top of the next page.

In this formula, $b_{h_i} = \sum_{j\in\mathcal{N}_{h_i}} a_{h_i,j} + a_{h_i,h_{i-1}}$, $i = 1,\ldots,t$, where h_0 represents the leader.

Define matrix $\hat{P}$ in the same formula with $\tilde{P}$ in (19).

1) Validity of $\hat{P}$: It is also not difficult to see that $c\sum_{j\in\mathcal{N}_1} a_{1j} - p + b_1 > 0$ holds in this scenario and obtain the following inequality based on (22), at the bottom of this page:

$$\lambda_{\min}\left\{\left(0.5\left(\hat{L}+\hat{L}^{\mathsf{T}}\right)\right)_{n-1}\right\} \geq \lambda_{\min}\{(L)_{n-1}\}.$$

Therefore, it is proved that $\hat{P}$ is positive definite.

2) Stability: Design the Lyapunov candidate as $\hat{V} = (1/2)\tilde{y}^{\mathsf{T}}(\hat{P}\otimes I_N)\tilde{y}$. We can also conclude that $\dot{\hat{V}}(t) \leq 0$, and $\dot{\hat{V}} = 0$ if and only if $\tilde{x} = 0$ and $\tilde{v} = 0$. By applying LaSalle's invariant principle, it guarantees that the tracking errors $\tilde{x}$ and $\tilde{v}$ of the entire system are globally asymptotically convergent to zero in this scenario. This completes the proof. ■

Remark 3: The constraint on the maximum tolerant magnitude of faults in (21) is less conservative than those in protocols B and C, which implies the fault-tolerant ability of the MVS is stronger in this scenario. It is reasonable because the faulty vehicle is more far away from the leader, and its impact would be diminished accordingly. In addition, the

$$\hat{L} = \begin{bmatrix} \sum\limits_{j\in\mathcal{N}_1} a_{1j} & \cdots & 0 & -a_{1,h_{t-2}} & \cdots & \cdots & \cdots & \cdots & -a_{1n} \\ \vdots & \ddots & \vdots & \vdots & \vdots & \vdots & \vdots & \vdots & \vdots \\ -a_{h_1,1} & \cdots & b_{h_1} & 0 & \cdots & \cdots & \cdots & \cdots & -a_{h_1,n} \\ \vdots & \vdots & \vdots & \ddots & \vdots & \vdots & \vdots & \vdots & \vdots \\ -a_{h_{t-2},1} & \cdots & \cdots & -a_{h_{t-2},h_{t-3}} & b_{h_{t-2}} & 0 & \cdots & \cdots & -a_{h_{t-2},n} \\ -a_{h_{t-1},1} & \cdots & \cdots & \cdots & -a_{h_{t-1},h_{t-2}} & b_{h_{t-1}} & 0 & \cdots & -a_{h_{t-1},n} \\ -\rho_0 a_{h1} & \cdots & \cdots & \cdots & \cdots & -\rho_0 a_{h,h_{t-1}} & \rho_0 b_{h_t} & \cdots & -\rho_0 a_{hn} \\ \vdots & \vdots & \vdots & \vdots & \vdots & \vdots & \vdots & \ddots & \vdots \\ -a_{n1} & \cdots & \cdots & \cdots & \cdots & \cdots & \cdots & \cdots & \sum\limits_{j\in\mathcal{N}_n} a_{nj} \end{bmatrix} \tag{22}$$

Algorithm 3 Integrated Topology Reconfiguration-Based FTCC Framework

Input: vehicle h, its layer number k and the information of ρ_0;

Output: conduct a proper topology reconfiguration protocol to achieve the fault tolerance objective;

if $k = 1$ **then**
  adjust b_1 as $\bar{b}_1 = \frac{1}{\rho_0} b_1 + \frac{1-\rho_0}{\rho_0} c \sum_{j \in \mathcal{N}_1} a_{1j}$;
else if $k = 2$ **then**
  call Algorithm 1;
else if $k = 3$ **then**
  build a new directed arc $(1, h)$, and set $a_{h1} = 2a_M$;
  adjust a_{jh} as $\bar{a}_{jh} = (2 - \rho_0) a_{jh}$, $j \in \mathcal{N}_h$;
else
  call Algorithm 2;
  adjust the connection weights according to Theorem 5;
end if

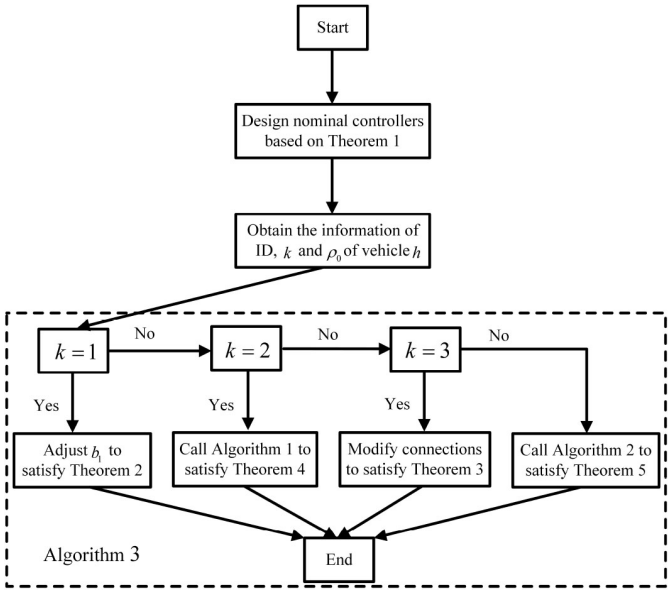

Fig. 3. Flow chart of the proposed FTCC framework.

proof of Theorem 5 follows the similar idea of Theorem 3. A directed path from the leader to the faulty vehicle h is built to provide more effort for the faulty one, and it would not affect the stability of the leader as well. Meanwhile, the weights a_{jh} ($j \in \mathcal{N}_h$) of the connections (h, j) are reset as the same values in Theorem 3 to exactly counteract the fault impact under the same principle.

V. Integrated Topology Reconfiguration-Based FTCC Framework

Based on the aforementioned topology reconfiguration protocols, an integrated topology reconfiguration-based FTCC framework is synthesized. Specifically, when a certain fault is detected, this FTCC framework is activated, then the predesigned protocol with respect to the detected fault operates. Algorithm 3 shows the details of the integrated FTCC framework, and its computational complexity is $O(n^2)$ as well. In addition, a flow chart is given in Fig. 3 to describe the internal logics of the proposed FTCC framework more clearly.

Based on all the constraints on the maximum tolerable magnitude of LoCE faults in protocols B–D and Algorithm 3, we can obtain the following theorem.

Theorem 6: For the MVS (4) with $\Gamma = I_{nm}$, design the original topology and nominal control laws (6) and (7) to satisfy Theorem 1 and Assumption 1. Consider vehicle h of this group encounters the partial LoCE faults described in (3), the maximum tolerable magnitude of which satisfies the following inequalities:

$$1 - \rho_0 \begin{cases} < 1, h = 1 \\ \leq \frac{a_M}{\sum_{j \in \mathcal{N}_h} a_{rj} + a_M} & \forall r \in \mathcal{C}_h(h), k = 2 \\ \leq \frac{a_M}{\sum_{j \in \mathcal{N}_h} a_{hj} + a_M}, & k = 3 \\ \leq \frac{2a_M}{\sum_{j \in \mathcal{N}_h} a_{hj}}, & k > 3 \end{cases} \tag{22}$$

where $\forall h \in \mathcal{V}$, and k represents the layer number of the faulty vehicle h. After the fault diagnosis, the information of the faults, including the ID and the layer number of the faulty vehicle, and the fault severity, has been obtained. By conducting Algorithm 3, the faulty MVS (4) can asymptotically track the references x_r and v_r generated by (5) with the original structure and design parameter of nominal control laws.

Proof: Since the stability analysis has been given for each fault scenario, the proof of Theorem 6 is omitted here. ■

For the realization of the proposed FTCC framework, since the topology reconfiguration protocols with respect to different fault scenarios have been predesigned, thus could be stored in the local supervisor of each vehicle. If each vehicle is equipped with one transmitter and one receiver, then it could adopt the broadcast communication to inform other vehicles within its communication range of the information, including its own ID, states, and fault severity through the transmitter. When a particular vehicle is faulty, some other vehicles are informed of this fault, and then would modify the information receiving actions through the receiver according to the corresponding protocol, for example, refuse to receive the information of the faulty one or tune the weight of that information. Meanwhile, the faulty vehicle would modify its own information receiving actions in a similar way.

Remark 4: It should be noted that Algorithms 1–3 are applied only after the fulfillment of the fault detection. As the FTCC framework only requires the lower bound of the LoCE fault as the fault information, unlike most existing controller reconfiguration-based methodologies, each vehicle under the proposed FTCC framework could only equip with basic state feedback-based controllers and simple fault diagnosis devices, the fault detection results of which are not required to be accurate. Thus, the fault detection is not the focus of this article, and readers can refer to [37]–[39] for details of fault diagnosis methodologies. In addition, if the detected faults with respect to the corresponding scenario exceed the maximum tolerable magnitude given in (18), (20), or (21), the proposed FTCC framework cannot guarantee the system stability and performance since high fault severity may lead to the unrecoverability of faults. To deal with those severe fault scenarios, Yang *et al.* [31] and Kamel *et al.* [32] have reported that the fault-tolerant capability of the MVS system can be achieved by

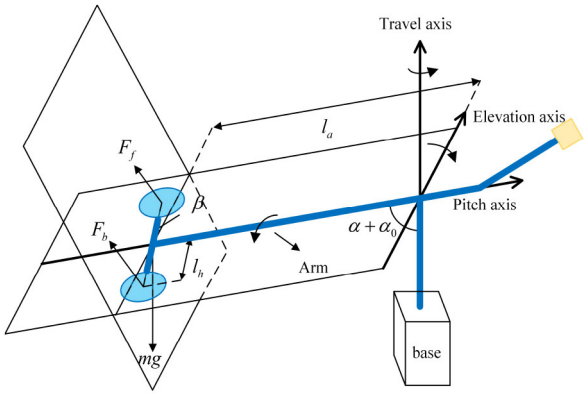

Fig. 4. Diagram of the 3-DOF helicopter.

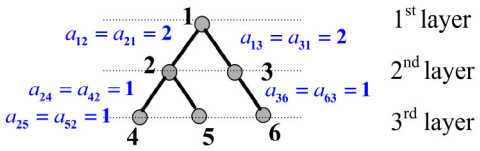

Fig. 5. Original topology implemented in the simulation.

removing the vehicle with heavy failures and simultaneously reorganizing the topology of the remaining healthy ones. Since this idea is not the focus of this article as well, further details would not be discussed.

Remark 5: The proposed topology reconfiguration-based FTCC framework is still effective in a directed spanning tree, since the original topology would be changed into a directed spanning tree by operating the developed topology reconfiguration protocols. Compared with the undirected spanning tree, the main difference in the directed one lies on the parameter selection of the nominal control laws. If the topology is originally designed as a directed spanning tree, the nominal control laws can still be designed as (6) and (7), but the left-hand side of (11) should be reformulated as $\lambda_{\min}\{(0.5(L+L^T))_{n-1}\}$ to achieve the asymptotical tracking performance in the fault-free scenario. Then, based on these modified nominal control laws, four high-level topology reconfiguration protocols designed in Section IV remain workable under different fault scenarios. To focus on the design of the FTCC framework, the original topology is set as an undirected spanning tree.

VI. Simulation Results

In this section, the simulations under different fault scenarios are conducted on six 3-DOF helicopter systems to verify the effectiveness of the proposed FTCC framework.

The 3-DOF helicopter (see Fig. 4) is a suitable platform for the study of fault-tolerant attitude synchronization of MVSs. By considering the pitch and elevation dynamics [40]–[42], the nonlinear model of the ith 3-DOF helicopter is in the same formula of (1), where $i=1,\ldots,6$, $x_i \triangleq [\alpha_i,\ \beta_i]^{\mathsf{T}} = [x_{i1}, x_{i2}]^{\mathsf{T}} \in \mathbb{R}^2$ and $v_i \in \mathbb{R}^2$ are elevation and pitch angles, and their rates of the ith helicopter, respectively. The input vector $u_i(\cdot)$ is defined as $u_i(\cdot) = [u_{fi},\ u_{bi}]^{\mathsf{T}}$, in which u_{fi} and u_{bi} represent the voltages of front and back motors, respectively. $f(x_i)$, $g(x_i)$

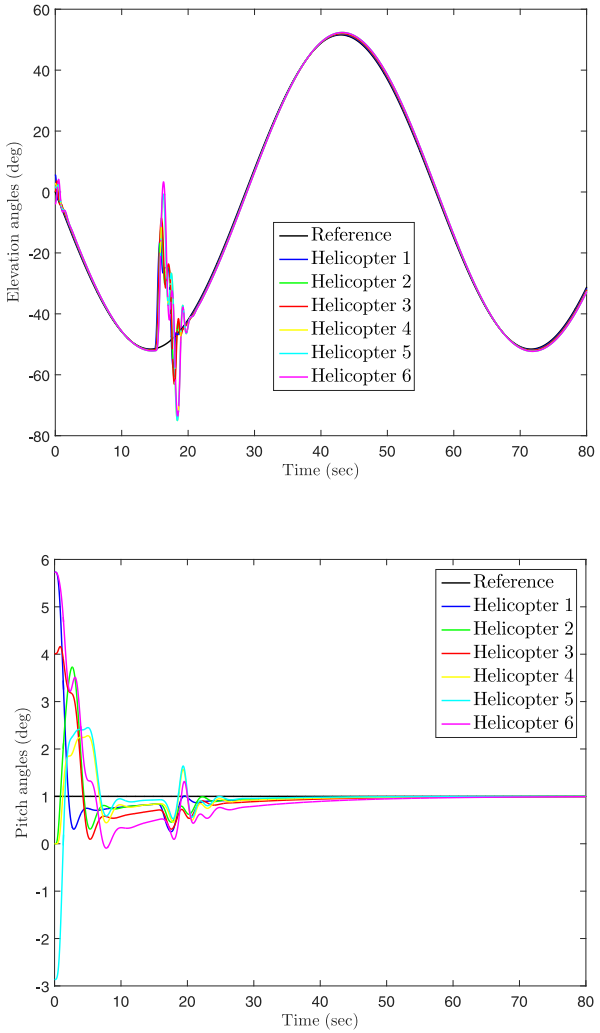

Fig. 6. Case 1: Trajectories of attitude angles versus time.

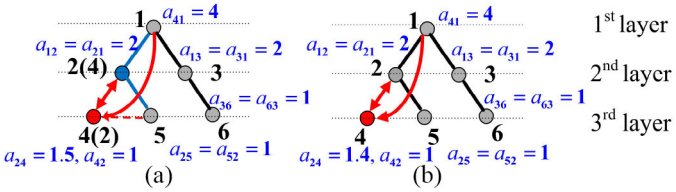

Fig. 7. Modified topologies: (a) in Case 2 and (b) in Case 3.

are given by

$$f(x_i) = \begin{bmatrix} -\left(mgl_a/J_e\right)\sin(\alpha_i+\alpha_{0i}) \\ 0 \end{bmatrix}$$

$$g(x_i) = \begin{bmatrix} K_f l_a \cos\beta_i/J_e & K_f l_a \cos\beta_i/J_e \\ K_f l_h/J_p & -K_f l_h/J_p \end{bmatrix}$$

where α_{0i} denotes the initial angle between the helicopter and the base. J_e, J_p are the moments of inertia with the respect to the elevation and pitch axes, respectively. K_f, m, and g are the force coefficient of the propeller, the effective mass, and the gravity, respectively. l_a and l_h are the distance from the travel axis to the helicopter body and the one from the pitch axis to each rotor, respectively.

The topology of the multihelicopter system is originally designed as an undirected spanning tree shown in Fig. 5,

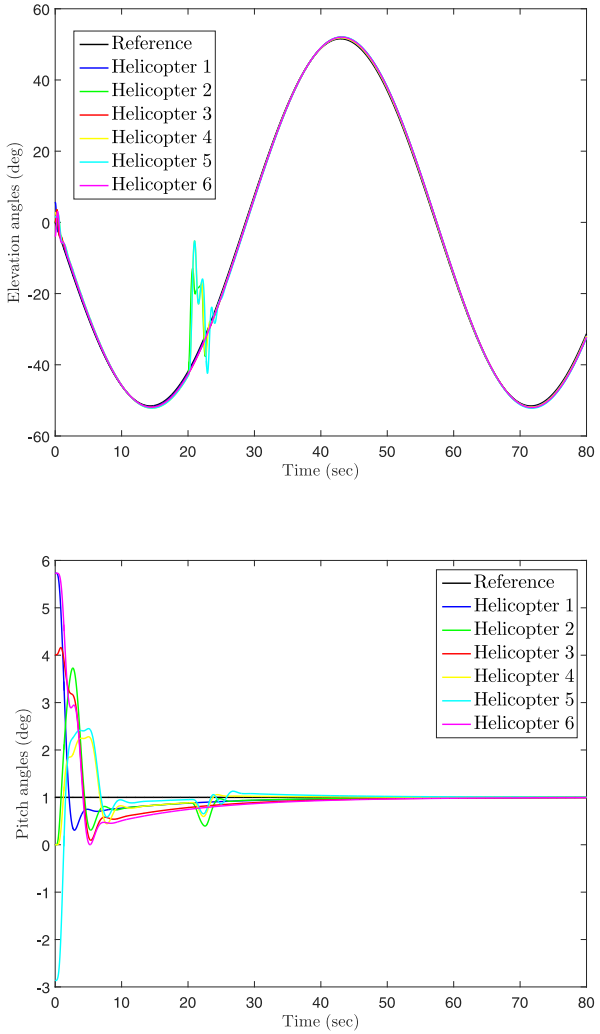

Fig. 8. Case 2: Trajectories of attitude angles versus time.

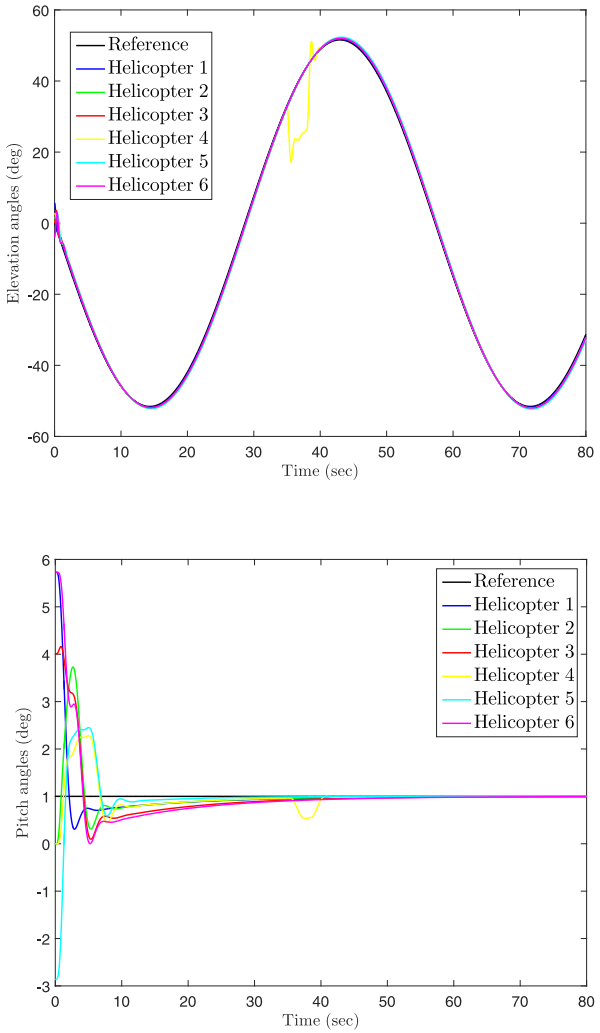

Fig. 9. Case 3: Trajectories of attitude angles versus time.

and satisfies Assumption 1. Each helicopter is marked with an unique ID and its layer number is also given in Fig. 5. The weights of the connections are initially selected as $a_{1j} = a_{j1} = 2$, $j \in \mathcal{N}_1$ and $a_{ij} = a_{ji} = 1$ for $\forall i \neq 1$, $j \in \mathcal{N}_i$, then we calculate that $\lambda_{\min}\{(L)_{n-1}\} = 0.4384$.

In this work, all the helicopters are assumed to be homogenous. The system parameters for each vehicle are given as

$$J_e = 1.004\ \left(\text{kg}\cdot\text{m}^2\right),\ J_p = 0.0445\ \left(\text{kg}\cdot\text{m}^2\right)$$
$$m = 0.142\ (\text{kg}),\ K_f = 0.625\ (\text{N/V})$$
$$l_a = 0.648\ (\text{m}),\ l_h = 0.178\ (\text{m}).$$

It is easy to verify that $f_k(x_i)$ $(i \in \mathcal{V},\ k = 1, 2)$ satisfy Assumption 2. Recalling (8), we have $p = 1.45$ when σ is selected as $\sigma = 0.5$. According to conditions (10) and (11), the parameter c and pinning gain b_1 are designed as $c = 6$ and $b_1 = 588$, respectively.

The initial attitude orientations of each helicopter are set as $x_{10} = [5.65, 5.65]^\mathsf{T}$ (deg), $x_{20} = [0, 0]^\mathsf{T}$ (deg), $x_{30} = [0, 4.95]^\mathsf{T}$ (deg), $x_{40} = [2.83, 0]^\mathsf{T}$ (deg), $x_{50} = [1.70, -2.83]^\mathsf{T}$ (deg), $x_{60} = [-4.95, 5.65]^\mathsf{T}$ (deg) and $v_{i0} = [0, 0]^\mathsf{T}$ (deg/sec) with $i = 1, \ldots, 6$. In addition, the initial states of the reference signals are given by $x_{r0} = [0, 1]^\mathsf{T}$ (deg) and $v_{r0} = [0, 0]^\mathsf{T}$ (deg/sec).

Case 1 (Leading Helicopter Is Faulty): In this case, suppose that all the helicopters operate normally from the beginning, then Helicopter 1 suffers a partial LoCE fault on the back motor with $\rho_1 = \text{diag}\{1, 0.5\}$ since 15 s. If it takes 2 s to accomplish the fault detection, the pinning gain b_1 would be tuned as 1200 since 17 s. As a result, Fig. 7 shows that the entire group can asymptotically track the reference signals in a synchronized way.

Case 2 (Child Node of the Leading Helicopter Is Faulty): Suppose that all the helicopters operate normally from the beginning, then Helicopter 2 suffers a partial LoCE fault on the front motor with $\rho_2 = \text{diag}\{0.5, 1\}$ since 20 s. If it takes 2 s to detect the fault, by applying Algorithm 3, the directed arc (2, 1) and the undirected one [2, 5] are deleted since 22 s. Simultaneously, two new undirected arcs [1, 4] and [4, 5] are built, and then Helicopters 4 and 2 exchange their IDs. By setting the weight a_{41} as $a_{41} = 4$ and modifying the weight a_{24} as $a_{24} = 1.5$ [see the modified topology in Fig. 7(a)], the fault tolerance objective can be achieved. It is shown in Fig. 8 that the synchronization and tracking performances of

the group are of satisfactory with the original structure and design parameter of nominal control laws in the presence of the faulty Helicopter 2.

Case 3 (Grandchild Node of the Leading Helicopter Is Faulty): In this case, consider another partial LoCE fault occurs on the back motor of Helicopter 4. Suppose that $\rho_4 = \text{diag}\{1, 0.6\}$ since 35 s and the fault detection of this fault accomplishes at 38 s. Then, by conducting Algorithm 3, a new directed arc (1, 4) is built, and its weight is set as $a_{41} = 4$. Meanwhile, the weight of a_{24} is adjusted as 1.4. The modified topology is shown in Fig. 7(b). Seen from Fig. 9, when the topology has been completely reconfigured, the performance of this multihelicopter group is recovered rapidly.

In general, all the simulation results illustrate that the multihelicopter system can achieve the attitude synchronization and asymptotically track the reference signals under the proposed FTCC framework even if it encounters various fault scenarios.

VII. Conclusion

For nonlinear MVSs with partial LoCE faults, a hierarchical FTCC framework that consists of the distributed nominal control scheme and the topology reconfiguration protocols has been proposed. The nominal control scheme, as the low-level one, has been developed to make each vehicle track the reference signals under a predesigned topology in the fault-free scenario. Based on it, the high-level topology reconfiguration protocols have been proposed to mitigate the fault impact. By applying the proposed FTCC framework, the topology has been adjusted through the corresponding protocol with respect to the ongoing fault scenario. As a result, asymptotical synchronization and reference tracking have been achieved with the original structure and design parameter of the nominal control scheme. The effectiveness of the proposed methodology has been verified through the simulation results on 3-DOF helicopter platforms. In the future investigations, the design of the formation reconfiguration-based FTCC framework that has the ability of handling more fault types and the design of the event-triggered FTCC framework [43], [44] will be explored.

References

[1] Y. Zhang and H. Mehrjerdi, "A survey on multiple unmanned vehicles formation control and coordination: Normal and fault situations," in *Proc. Int. Conf. Unmanned Aircraft Syst. (ICUAS)*, Atlanta, GA, USA, 2013, pp. 1087–1096.

[2] Z. Lin, M. Broucke, and B. Francis, "Local control strategies for groups of mobile autonomous agents," *IEEE Trans. Autom. Control*, vol. 49, no. 4, pp. 622–629, Apr. 2004.

[3] B. Zhu, H. H.-T. Liu, and Z. Li, "Robust distributed attitude synchronization of multiple three-DOF experimental helicopters," *Control Eng. Pract.*, vol. 36, pp. 87–99, Mar. 2015.

[4] J. R. Lawton and R. W. Beard, "Synchronized multiple spacecraft rotations," *Automatica*, vol. 38, no. 8, pp. 1359–1364, 2002.

[5] W. Ren, "Multi-vehicle consensus with a time-varying reference state," *Syst. Control Lett.*, vol. 56, nos. 7–8, pp. 474–483, 2007.

[6] Z. Qu, J. Wang, and R. A. Hull, "Cooperative control of dynamical systems with application to autonomous vehicles," *IEEE Trans. Autom. Control*, vol. 53, no. 4, pp. 894–911, May 2008.

[7] W. Ren, "Distributed cooperative attitude synchronization and tracking for multiple rigid bodies," *IEEE Trans. Control Syst. Technol.*, vol. 18, no. 2, pp. 383–392, Mar. 2010.

[8] D. V. Dimarogonas, P. Tsiotras, and K. J. Kyriakopoulos, "Leader–follower cooperative attitude control of multiple rigid bodies," *Syst. Control Lett.*, vol. 58, no. 6, pp. 429–435, 2009.

[9] X. Su, F. Xia, J. Liu, and L. Wu, "Event-triggered fuzzy control of nonlinear systems with its application to inverted pendulum systems," *Automatica*, vol. 94, no. 94, pp. 236–248, 2018.

[10] S. Azizi and K. Khorasani, "Cooperative actuator fault accommodation in formation flight of unmanned vehicles using absolute measurements," *IET Control Theory Appl.*, vol. 6, no. 18, pp. 2805–2819, Dec. 2012.

[11] S. Azizi and K. Khorasani, "Cooperative actuator fault accommodation in formation flight of unmanned vehicles using relative measurements," *Int. J. Control*, vol. 84, no. 5, pp. 876–894, 2011.

[12] M. M. Tousi and K. Khorasani, "Optimal hybrid fault recovery in a team of unmanned aerial vehicles," *Automatica*, vol. 48, no. 2, pp. 410–418, 2012.

[13] E. Semsar-Kazerooni and K. Khorasani, "Team consensus for a network of unmanned vehicles in presence of actuator faults," *IEEE Trans. Control Syst. Technol.*, vol. 18, no. 5, pp. 1155–1161, Sep. 2010.

[14] Z. Gallehdari, N. Meskin, and K. Khorasani, "A distributed control reconfiguration and accommodation for consensus achievement of multiagent systems subject to actuator faults," *IEEE Trans. Control Syst. Technol.*, vol. 24, no. 6, pp. 2031–2047, Nov. 2016.

[15] X. Yu, Z. Liu, and Y. Zhang, "Fault-tolerant formation control of multiple UAVs in the presence of actuator faults," *Int. J. Robust Nonlinear Control*, vol. 26, no. 12, pp. 2668–2685, 2016.

[16] B. Zhou, W. Wang, and H. Ye, "Cooperative control for consensus of multi-agent systems with actuator faults," *Comput. Elect. Eng.*, vol. 40, no. 7, pp. 2154–2166, 2014.

[17] H. Yang, C. Huang, B. Jiang, and M. M. Polycarpou, "Fault estimation and accommodation of interconnected systems: A separation principle," *IEEE Trans. Cybern.*, vol. 49, no. 12, pp. 4103–4116, Dec. 2019.

[18] C. Liu, B. Jiang, R. J. Patton, and K. Zhang, "Decentralized output sliding-mode fault-tolerant control for heterogeneous multiagent systems," *IEEE Trans. Cybern.*, early access, May 6, 2019, doi: 10.1109/TCYB.2019.2912636.

[19] J. Li and K. D. Kumar, "Decentralized fault-tolerant control for satellite attitude synchronization," *IEEE Trans. Fuzzy Syst.*, vol. 20, no. 3, pp. 572–586, Jun. 2012.

[20] Y. Wang, Y. Song, and F. L. Lewis, "Robust adaptive fault-tolerant control of multiagent systems with uncertain nonidentical dynamics and undetectable actuation failures," *IEEE Trans. Ind. Electron.*, vol. 62, no. 6, pp. 3978–3988, Jun. 2015.

[21] J. Qin, G. Zhang, W. X. Zheng, and Y. Kang, "Adaptive sliding mode consensus tracking for second-order nonlinear multiagent systems with actuator faults," *IEEE Trans. Cybern.*, vol. 49, no. 5, pp. 1605–1615, May 2019.

[22] A. Dorri, S. S. Kanhere, and R. Jurdak, "Multi-agent systems: A survey," *IEEE Access*, vol. 6, pp. 28573–28593, 2018.

[23] Q. Shan, J. Yan, T. Li, and C. P. Chen, "Containment control of multi-agent systems with general noise based on hierarchical topology reconfiguration," *IEEE Access*, vol. 7, pp. 56826–56838, 2019.

[24] B. Zhao, Y. Guan, and L. Wang, "Controllability improvement for multiagent systems: Leader selection and weight adjustment," *Int. J. Control*, vol. 89, no. 10, pp. 2008–2018, 2016.

[25] D. Maithripala and S. Jayasuriya, "Rigid formation keeping and formation reconfiguration of multi-agent systems," *IFAC Proc. Vol.*, vol. 41, no. 2, pp. 5155–5160, 2008.

[26] M. T. Nguyen, C. S. Maniu, S. Olaru, and A. Grancharova, "Fault tolerant predictive control for multi-agent dynamical systems: Formation reconfiguration using set-theoretic approach," in *Proc. Int. Conf. Control Decis. Inf. Technol.*, Metz, France, 2014, pp. 417–422.

[27] S. Yoon and J. Kim, "Efficient multi-agent task allocation for collaborative route planning with multiple unmanned vehicles," *IFAC-PapersOnLine*, vol. 50, no. 1, pp. 3580–3585, 2017.

[28] H. Yang, Q.-L. Han, X. Ge, L. Ding, Y. Xu, B. Jiang, and D. Zhou, "Fault-tolerant cooperative control of multiagent systems: A survey of trends and methodologies," *IEEE Trans. Ind. Informat.*, vol. 16, no. 1, pp. 4–17, Jan. 2020.

[29] H. Yang, M. Staroswiecki, B. Jiang, and J. Liu, "Fault tolerant cooperative control for a class of nonlinear multi-agent systems," *Syst. Control Lett.*, vol. 60, no. 4, pp. 271–277, 2011.

[30] I. Saboori and K. Khorasani, "Actuator fault accommodation strategy for a team of multi-agent systems subject to switching topology," *Automatica*, vol. 62, pp. 200–207, Dec. 2015.

[31] H. Yang, B. Jiang, and H. Yang, "Fault tolerant cooperative control for multiple unmanned aerial vehicle systems with plugging operations," *Proc. Inst. Mech. Eng. I, J. Syst. Control Eng.*, vol. 230, no. 8, pp. 820–829, 2016.

[32] M. A. Kamel, X. Yu, and Y. Zhang, "Fault-tolerant cooperative control design of multiple wheeled mobile robots," *IEEE Trans. Control Syst. Technol.*, vol. 26, no. 2, pp. 756–764, Mar. 2018.
[33] K. Yong, M. Chen, and Q. Wu, "Immersion and invariance-based integrated guidance and control for unmanned aerial vehicle path following," *Int. J. Syst. Sci.*, vol. 50, no. 5, pp. 1052–1068, 2019.
[34] Q. Song and J. Cao, "On pinning synchronization of directed and undirected complex dynamical networks," *IEEE Trans. Circuits Syst. I, Reg. Papers*, vol. 57, no. 3, pp. 672–680, Mar. 2010.
[35] X. Zhan, "Extremal eigenvalues of real symmetric matrices with entries in an interval," *SIAM J. Matrix Anal. Appl.*, vol. 27, no. 3, pp. 851–860, 2005.
[36] H. Khalil, *Nonlinear Systems*, 3rd ed. Upper Saddle River, NJ, USA: Prentice-Hall, 2002.
[37] R. J. Patton, P. M. Frank, and R. N. Clark, *Issues of Fault Diagnosis for Dynamic Systems*. London, U.K.: Springer, 2000.
[38] X. Zhang, M. M. Polycarpou, and T. Parisini, "Fault diagnosis of a class of nonlinear uncertain systems with Lipschitz nonlinearities using adaptive estimation," *Automatica*, vol. 46, no. 2, pp. 290–299, 2010.
[39] K. Zhang, B. Jiang, and P. Shi, "Distributed fault estimation observer design with adjustable parameters for a class of nonlinear interconnected systems," *IEEE Trans. Cybern.*, vol. 49, no. 12, pp. 4219–4228, Dec. 2019.
[40] B. Zheng and Y. Zhong, "Robust attitude regulation of a 3-DOF helicopter benchmark: Theory and experiments," *IEEE Trans. Ind. Electron.*, vol. 58, no. 2, pp. 660–670, Feb. 2011.
[41] Z. Li, J. Yu, X. Xing, and H. Gao, "Robust output-feedback attitude control of a three-degree-of-freedom helicopter via sliding-mode observation technique," *IET Control Theory Appl.*, vol. 9, no. 11, pp. 1637–1643, Jul. 2015.
[42] J. Shan, H.-T. Liu, and S. Nowotny, "Synchronised trajectory-tracking control of multiple 3-DOF experimental helicopters," *Proc. Inst. Elect. Eng.,, Control Theory Appl.*, vol. 152, no. 6, pp. 683–692, Nov. 2005.
[43] X. Liu, X. Su, P. Shi, C. Shen, and Y. Peng, "Event-triggered sliding mode control of nonlinear dynamic systems," *Automatica*, vol. 112, no. 112, 2020, Art. no. 108738.
[44] X. Su, X. Liu, P. Shi, and Y. Song, "Sliding mode control of hybrid switched systems via an event-triggered mechanism," *Automatica*, vol. 90, no. 90, pp. 294–303, 2018.

Huiliao Yang (Member, IEEE) was born in Chengdu, China, in 1990. She received the B.S. and Ph.D. degrees in automatic control from the Nanjing University of Aeronautics and Astronautics, Nanjing, China, in 2012 and 2019, respectively.

She is currently an Assistant Professor with the College of Energy and Electrical Engineering, Hohai University, Nanjing. Her research interests include fault-tolerant cooperative control of multiagent systems and its application to UAVs.

Bin Jiang (Fellow, IEEE) received the Ph.D. degree in automatic control from Northeastern University, Shenyang, China, in 1995.

He was a Postdoctoral Fellow, a Research Fellow, an Invited Professor, and a Visiting Professor in Singapore, France, USA, and Canada, respectively. He is currently the Chair Professor of Cheung Kong Scholar Program with the Ministry of Education and the Vice President of the Nanjing University of Aeronautics and Astronautics, Nanjing, China. His current research interests include fault diagnosis, fault-tolerant control, and their applications in aircraft, satellite, and high-speed trains.

Prof. Jiang was a recipient of the First Class Prize of Natural Science Award of Ministry of Education of China in 2015, and the Second Class Prize of National Natural Science Award of China in 2018. He currently serves as an Associate Editor or an Editorial Board Member for a number of journals, such as the IEEE TRANSACTIONS ON CONTROL SYSTEMS TECHNOLOGY, the IEEE TRANSACTIONS ON CYBERNETICS, *International Journal of Control, Automation and Systems*, *Journal of Astronautics*, *Control and Decision*, and *Systems Engineering and Electronics Technologies*. He is the Chair of Control Systems Chapter in IEEE Nanjing Section, a Member of the IFAC Technical Committee on Fault Detection, Supervision, and Safety of Technical Processes.

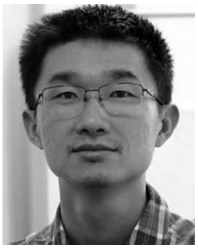

Hao Yang (Senior Member, IEEE) received the B.Sc. degree in electrical automation from Nanjing Tech University, Nanjing, China, in 2004, and the Ph.D. degrees in automatic control from the Universit de Lille 1: Sciences et Technologies, Lille, France, and the Nanjing University of Aeronautics and Astronautics (NUAA), Nanjing, in 2009.

Since 2010, he has been working with the College of Automation Engineering, NUAA, where he has been a Full Professor since 2015. He has published two books and over 80 international journal papers. His research interest includes control, optimization, and fault tolerance of switched, interconnected, and multiagent network systems with their aerospace applications.

Prof. Yang was a recipient of the National Science Fund of China for Excellent Young Scholars in 2016, and the Top-Notch Young Talents of Central Organization Department of China in 2017. He has served as an Associate Editor for *Nonlinear Analysis: Hybrid Systems*, *Cyber-Physical Systems*, *Acta Automatica Sinica*, and *Chinese Journal of Aeronautics*. He is also a Member of the IFAC Technical Committee on Fault Detection, Supervision and Safety of Technical Processes.

Hugh H. T. Liu (Member, IEEE) received the bachelor's degree in automatic control from Shanghai Jiao Tong University, Shanghai, China, in 1991, the master's degree in flight control and simulation from the Beijing University of Aeronautics and Astronautics, Beijing, China, in 1994, and the Ph.D. degree in mechanical engineering from the University of Toronto, Toronto, ON, Canada, in 1998.

He is currently a Professor with the Institute for Aerospace Studies, University of Toronto, where he has been a Faculty Member since 2000, and the Director of the Natural Science and Engineering Research Council of Canada-Collaborative Research and Training Experience Program on Unmanned Aerial Vehicles and the Centre for Aerial Robotics Research and Education. His research interests are in the areas of aircraft systems and control, including autonomous unmanned systems, cooperative and formation control, fault-tolerant control, active control on advanced aircraft systems, as well as integrated modeling and simulations.

Prof. Liu currently serves as an Associate Editor for the *AIAA Journal of Guidance, Control and Dynamics* and *Canadian Aeronautics and Space Journal*. He is a Fellow of the Engineering Institute of Canada and the Canadian Society of Mechanical Engineers, an Associate Fellow of AIAA, and a Registered Professional Engineer in Ontario, Canada.